JACS
JOURNAL OF THE AMERICAN CHEMICAL SOCIETY
Article
pubs.acs.org/JACS

Chiral Conjugated Corrals

Melissa Ball,[†,⊥] Brandon Fowler,[†,⊥] Panpan Li,[†,‡] Leo A. Joyce,[§] Fang Li,[‡] Taifeng Liu,[‡] Daniel Paley,[†] Yu Zhong,[†] Hexing Li,[*,‡] Shengxiong Xiao,[*,‡] Fay Ng,[*,†] Michael L. Steigerwald,[*,†] and Colin Nuckolls[*,†,‡]

[‡]The Education Ministry Key Lab of Resource Chemistry, Shanghai Key Laboratory of Rare Earth Functional Materials, Optoelectronic Nano Materials and Devices Institute, Department of Chemistry, Shanghai Normal University, Shanghai, China 200234

[†]Department of Chemistry, Columbia University, New York, New York 10027, United States

[§]Process and Analytical Chemistry, Merck Research Laboratories, Rahway, New Jersey 07065, United States

Supporting Information

ABSTRACT: We present here a new design motif for strained, conjugated macrocycles that incorporates two different aromatics into the cycle with an −A−B−A−B− pattern. In this study, we demonstrate the concept by alternating electron donors and acceptors in a conjugated cycle. The donor is a bithiophene, and the acceptor is a perylene diimide derivative. The macrocycle formed has a persistent elliptiform cavity that is lined with the sulfur atoms of the thiophenes and the π-faces of the perylene diimide. Due to the linkage of the perylene diimide subunits, the macrocycles exist in both chiral and achiral forms. We separate the three stereoisomers using chiral high-performance liquid chromatography and study their interconversion. The mechanism for interconversion involves an "intramolecular somersault" in which one of the PDIs rotates around its transverse axis, thereby moving one of its diimide heads through the plane of the cavity. These unusual macrocycles are black in color with an absorption spectrum that spans the visible range. Density functional theory calculations reveal a photoinduced electron transfer from the bithiophene to the perylene diimide.

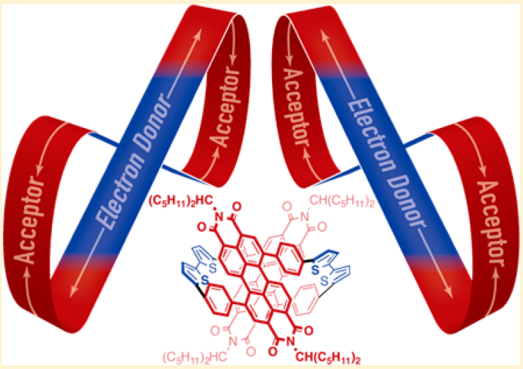

INTRODUCTION

This article describes the design, synthesis, and study of a new type of conjugated aromatic macrocycle formed from the linkage of donor and acceptor subunits into a strained cycle. These macrocycles are members of an ever-growing class of cyclic, conjugated belts, such as cycloparaphenylenes (CPPs)[1−17] and cycloporphyrins (CPs).[18−20] CPPs consist of para-connected phenylene rings and possess size-dependent optical and electronic properties.[11,21−23] However, CPPs do not absorb at a sufficiently broad part of the visible spectrum for them to be useful in optoelectronic devices.[24] The optical gaps for CPs are smaller, but they have not been studied in devices. There are no fully conjugated CPPs or CPs with two different aromatic subunits in an −A−B−A−B− pattern. Alternation of electron-donor and -acceptor subunits is a proven strategy to engineer the energetics of linear, conjugated oligomers and polymers,[25−27] but it has not been explored in the context of conjugated, cyclic oligomers. For this study, we designed and synthesized the molecules shown in Figure 1A, comprising two diphenyl perylene diimides (PDIs) and two bithiophenes. Each of these macrocycles has a persistent elliptiform cavity that is lined with electron-deficient π-faces of the PDI and the lone pairs of the sulfur atoms from the thiophene subunits. We have named these macrocycles "conjugated corrals" (abbreviated **CC1**). The corrals are black in color and have a broad absorption spectrum that spans the entire visible range. The onset of strong absorbance occurs at approximately 700 nm (HOMO-to-LUMO excitation at 1.8 eV), hinting at **CC1**'s favorable prospects as optical materials. Furthermore, we find that **CC1** exists in a dynamical equilibrium between both chiral [(*R*,*R*)-**CC1** and (*S*,*S*)-**CC1**] and meso [(*S*,*R*)-**CC1**] forms due to the handedness of the helical PDI subunits (Figure 1). The essential point of this study is that this new −A−B−A−B− motif for cyclic conjugated molecules (Figure 1A) provides interesting chiral information and an unusual electronic structure.

RESULTS AND DISCUSSION

We incorporated PDI as the electron acceptor in **CC1**'s design because PDI derivatives have shown a number of desirable behaviors: (1) they are efficient materials in n-type organic field effect transistors;[28] (2) they have high molar absorptivities;[29−31] (3) they are efficient electron acceptors in organic photovoltaics;[32−35] (4) they form small band gap polymers with electron-donating moieties; and (5) they are easily

Received: June 2, 2015
Published: July 30, 2015

DOI: 10.1021/jacs.5b05698
J. Am. Chem. Soc. 2015, 137, 9982−9987

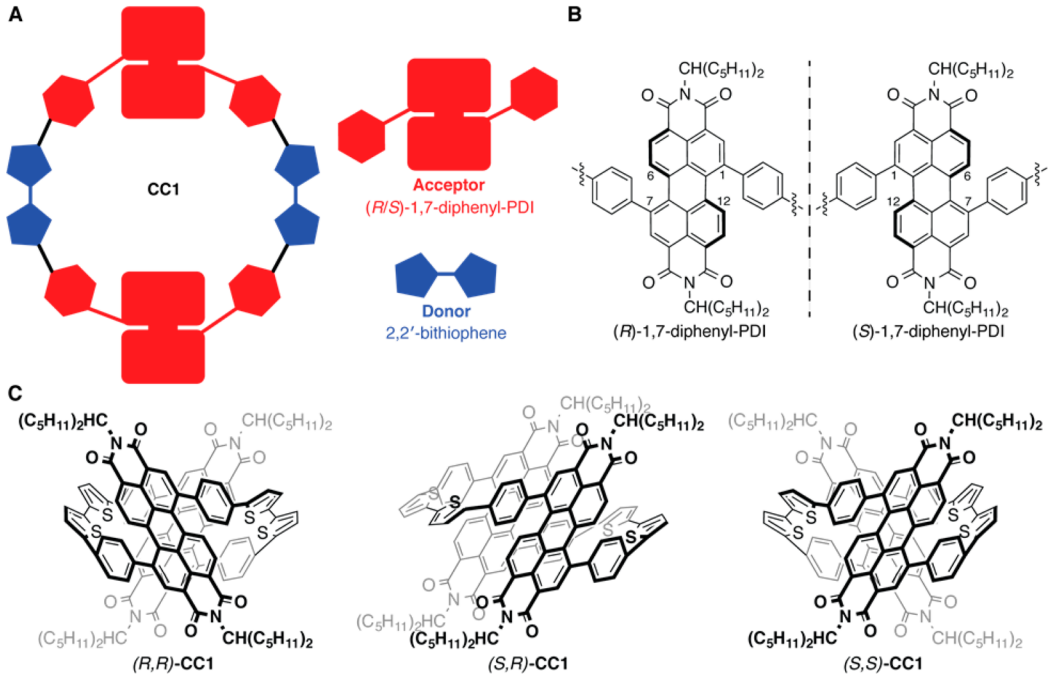

Figure 1. (A) Schematic structure of the −A−B−A−B− pattern encoded in **CC1**. (B) Stereoisomerism of **CC1** results from the chirality of the (*R*)- and (*S*)-1,7-diphenyl-PDI subunits. (C) Molecular, conjugated corrals (**CC**s) exist in chiral [(*R*,*R*)-**CC1** and (*S*,*S*)-**CC1**] and meso [(*S*,*R*)-**CC1**] forms.

Scheme 1. Synthesis of CC1[a]

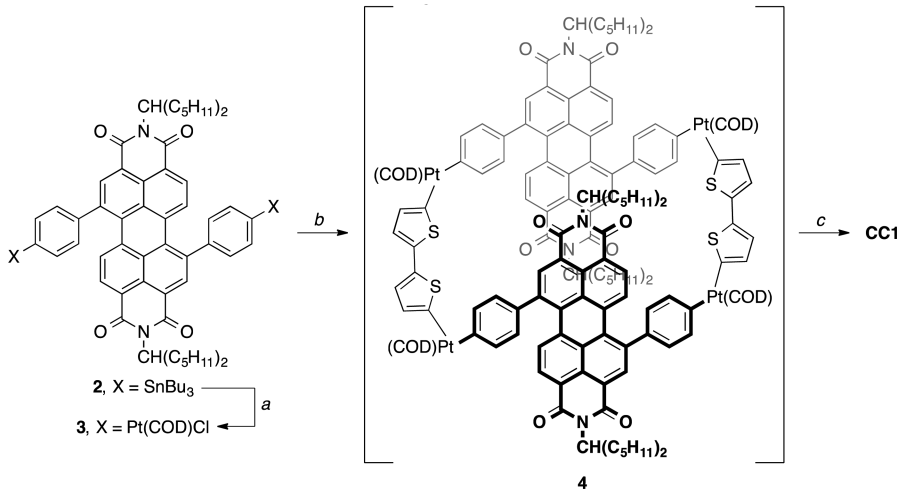

[a]Key: (a) $Pt(COD)Cl_2$, toluene, 100 °C, 24.5 h, 45% yield; (b) 5,5′-bis(trimethylstannyl)-2,2′-bithiophene, THF, 50 °C, 40 h; (c) PPh_3, toluene, 100 °C, 24 h, 8% yield (2 steps).

functionalized from inexpensive starting materials.[36,37] We employed oligothiophenes as the electron-rich counterpart because they are ubiquitous as electron-donor molecules in electronic materials.[38,39] Our synthesis is based on the strategies developed by Bäuerle[40] and Yamago[11,12] in the syntheses of conjugated macrocyles via square planar platinum intermediates.

Scheme 1 displays the synthesis of **CC1** that employs a four-cornered tetraplatinum macrocycle, **4**. The key intermediate is the bisplatinated diphenyl-PDI, **3**. We synthesize this important building block by a double Stille coupling[41,42] of 1,4-bis(tributylstannyl)benzene with the 1,7-dibromo-PDI[43−45] to afford the bis-tributyltin-substituted aromatic, **2**.[46] Transmetalation of **2** with dichloro(1,5-cyclooctadiene)platinum(II) provides **3**.[11] We heat equimolar amounts of **3** and 5,5′-bis(trimethylstannyl)-2,2′-bithiophene for 40 h to yield **4**. This organometallic macrocycle proved difficult to isolate, so we carried the crude material onto the ultimate product by heating it with excess triphenylphosphine. This initiates the 4-fold reductive elimination that forms **CC1**.[10] Preparative high-performance liquid chromatography (HPLC) gives pure **CC1** in an 8% yield from **3**. This yield is exceptional given that it incorporates two steps and provides such a complex strained macrocycle.

Scrambling of aryl−tin/aryl−platinum bonds has been observed in the formation of platinum macrocycles from unsubstituted aromatics;[11,12] however, Eaborn and co-workers found that scrambling was less pronounced when aryl groups

DOI: 10.1021/jacs.5b05698
J. Am. Chem. Soc. 2015, 137, 9982−9987

possessed electron-withdrawing substituents.[47] We sought to circumvent this scrambling by performing transmetalation on the PDI (**2** to **3**) prior to adding the electron-rich bithiophene subunit. In fact, upon isolating **3**, we find no evidence of scrambling of the Pt−phenyl bond when heated to 50 °C with tributyltin chloride for 48 h. This lack of reversibility is a new design feature that allows the synthesis, for the first time, of conjugated macrocycles with an alternating −A−B−A−B− pattern.

The branched undecyl side chains[48,49] and the molecular dynamics of the PDIs in **CC1** (vide infra) hinder formation of crystals suitable for single-crystal X-ray diffraction. High-resolution mass spectrometry (Supporting Information Figure S1A,B) confirms a cyclic structure that consists of two bithiophenes and two diphenyl-PDIs. The ^{1}H NMR spectrum of **CC1** contains several broad peaks in the aromatic region at room temperature, suggesting that the dynamical processes (rotation of the phenyl rings and the undecyl side chains)[50] occur on the NMR time scale (Figure S1C). Acquiring the NMR data at 87 °C (in 1,1,2,2-tetrachloroethane-d_2), however, provides a well-resolved ^{1}H NMR spectrum (Figure S1D). In the downfield region of the spectrum (Figure 2A), we observe

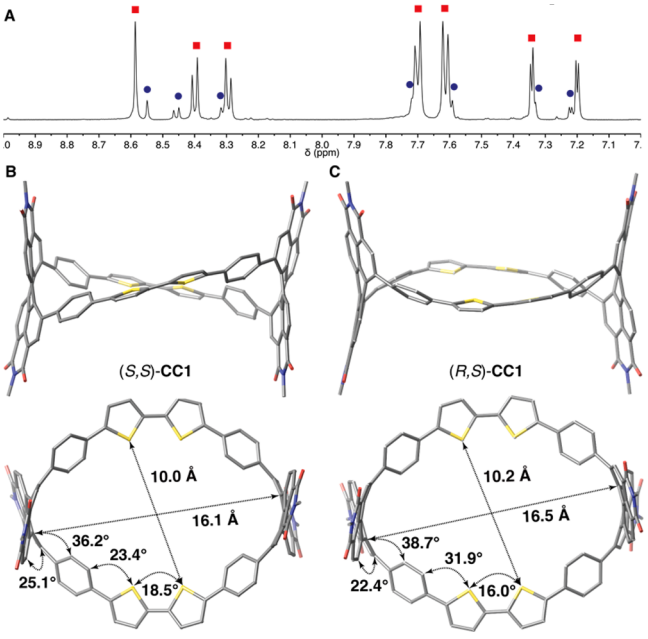

Figure 2. (A) Downfield region of the ^{1}H NMR spectrum of macrocycle **CC1** recorded at 87 °C. The red squares (chiral) and blue circles (achiral) identify resonances from the two stereoisomers. (B) DFT-minimized model (side-on and face-on views) of chiral stereoisomer (*S*,*S*)-**CC1** (undecyl side chains have been truncated to a methyl group to simplify the calculations). (C) DFT-minimized model (side-on and face-on views) of meso stereoisomer (*R*,*S*)-**CC1** (undecyl side chains have been truncated to a methyl group to simplify the calculations). Carbon = gray, nitrogen = blue, oxygen = red, sulfur = yellow. Hydrogens have been removed to clarify the view.

resonances consistent with the macrocycle alongside a smaller set of resonances that have analogous splitting and multiplicity. This pattern suggests that **CC1** exists as two closely related isomers, and integration of the resonances reveals that the two isomers occur in a ratio of approximately 6:1 (at 87 °C). The gas-phase calculations provide a ratio of 316:1 at 87 °C (see the Supporting Information for details). The effects of the medium, solvation, guest inclusion, and dielectric constant must account for the difference between calculated and observed ratios. We also performed variable-temperature NMR and did not observe coalescence up to 147 °C.

The two sets of resonances we observe in the NMR in Figure 2A are a result of stereoisomerism. The diphenyl-PDI moiety, when linked in the 1,7-position and constrained in a macrocycle, introduces chirality (Figure 1B). We were able to grow crystals of *N*,*N*′-di(6-undecyl)-1,7-di(4-bromophenyl)-perylene-3,4:9,10-tetracarboxylic diimide that revealed that the PDI core is highly contorted such that the long axis of the PDI is twisted into a helix, with a 22° dihedral angle between the two naphthalene subunits of the perylene.[51] This contorted core places each of the pendant aromatic rings on the same face of the PDI (Figure S2). This structural feature was observed previously in crystallography of PDIs substituted with ferrocene groups in the 1,7-positions.[52] With this information in hand, we used density functional theory (DFT) to determine energy-optimized structures for the stereoisomers, and these are represented in Figure 2B,C. When linked together by a pair of bithiophenes, two diphenyl-PDI subunits possessing the same chirality produce a pair of enantiomers [(*R*,*R*)-**CC1** and (*S*,*S*)-**CC1**, Figure 2B]. Alternatively, linking two PDI subunits with opposite chirality produces an achiral, meso form [(*R*,*S*)-**CC1**, Figure 2C]. The enantiomeric forms of **CC1** have an approximate C_2 axis that relates the two PDIs in the macrocycle. The achiral, meso isomer contains a mirror plane between the two PDIs. Both the chiral and meso forms of **CC1** have PDI core structures that resemble the diphenyl-PDI conformation. The twist of the PDI core in the meso isomer is the same as that of the diphenyl-PDI derivative, 22° (Figure S2), whereas the chiral isomer has a larger twist in its PDI subunit (25°, shown in Figure 2B). We believe that this twist and orientation of the phenyls facilitates formation of **CC1** by giving curvature to the otherwise flat PDI.

In both stereoisomers of **CC1**, the macrocycle has a persistent elliptiform cavity, measuring 1.6 nm from PDI to PDI and 1.0 nm from bithiophene to bithiophene. One striking difference between these two stereoisomers is the apparent strain in the tetracyclic linkers connecting the PDIs. The meso isomer forces the linkers to bow in order to accommodate the rigidity of the cycle (Figure 2C), while in the chiral isomer, the tetracyclic linkers are essentially flat (Figure 2B), which make the chiral isomer appear less strained. In both isomers, the sulfur atoms of the four thiophenes point into the cavity, while the diphenyl-PDIs cap the ends of the macrocycle. Oligothiophenes typically possess an antigeometry of their sulfur atoms rather than syn orientation, reflecting decreased steric repulsion in the former.[53−55] However, this is not the case for **CC1**. The bithiophene orientation plays a crucial role in the assembly of **CC1** by relieving strain. In order to quantify this effect, we modeled the syn and anti conformers of simple bithiophene, $C_8H_6S_2$. The angle between the two terminal C−H bond vectors defines the curvature supported by the bithiophene. This angle is 117° in the syn geometry and 180° in the anti geometry. Thus, the syn orientation of the bithiophene promotes the formation and stabilization of **CC1**. Conversely, the incorporation of the bithiophenes into **CC1** promotes the otherwise unfavorable syn orientation in the bithiophenes. Reports from Bäuerle and Itami describe a similar conformation preference in macrocyclic, 2,5-linked oligothiophenes.[40,56] Calculations using a homodesmotic reaction reveal that the strain energy is ∼20 kcal/mol for the chiral isomers of

DOI: 10.1021/jacs.5b05698
J. Am. Chem. Soc. 2015, 137, 9982−9987

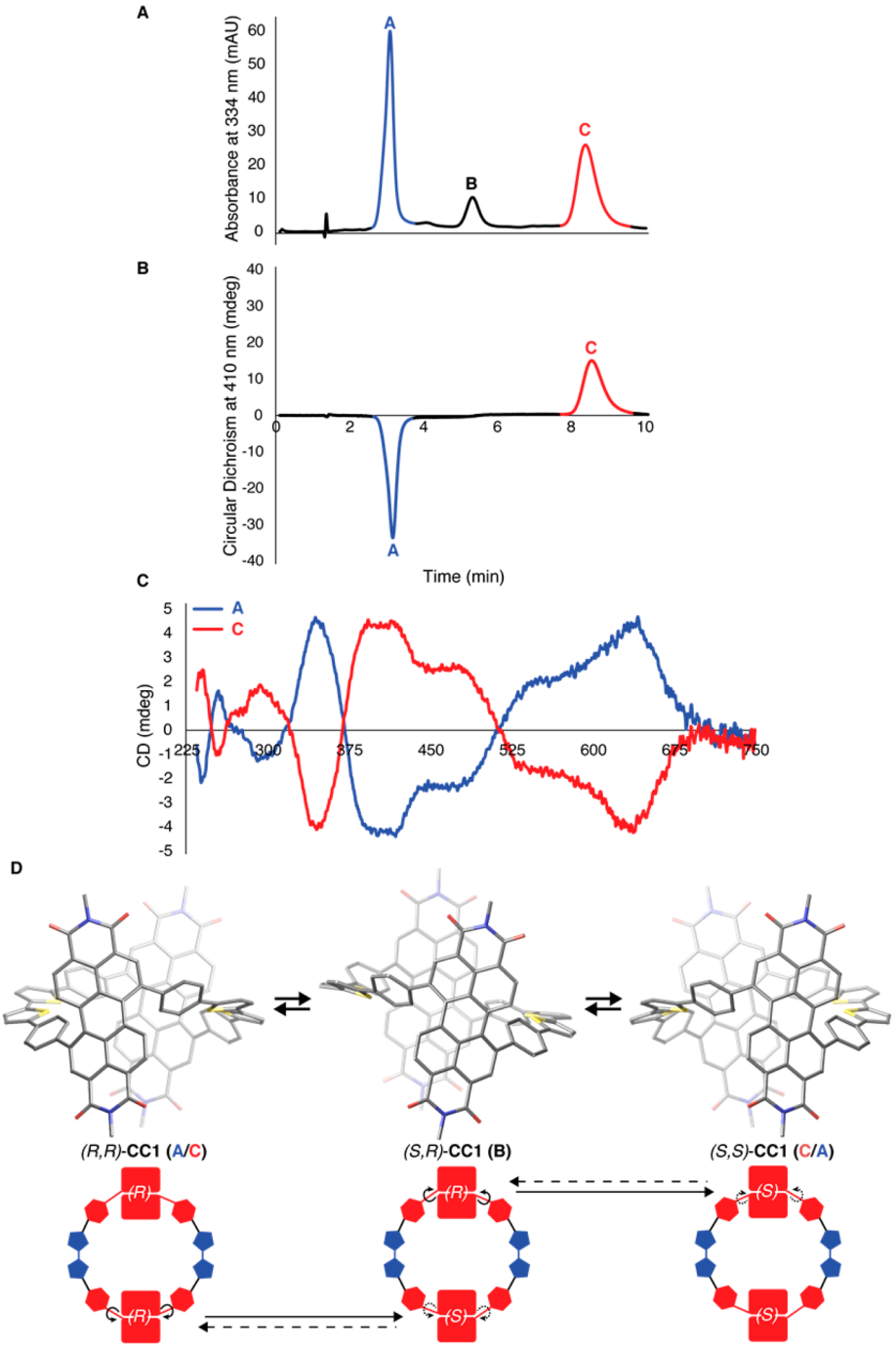

Figure 3. (a) HPLC chromatogram of **CC1** using a CHIRALPAK IA-3 column. (b) HPLC-CD chromatogram of **CC1** showing that peaks **A** and **C** exhibit opposite optical activity (270−410 nm). (c) CD spectra for both enantiomers of **CC1**. (D) Interconversion of the stereoisomers of **CC1** by sequential rotation of one PDI subunit through the macrocycle and then rotation of the other PDI to convert between enantiomers. The hydrocarbon side chains have been replaced with a methyl group. Carbon = gray, nitrogen = blue, oxygen = red, sulfur = yellow. Hydrogen atoms have been removed to clarify the view.

CC1 and 22 kcal/mol for the meso isomer. The Supporting Information contains the details of these calculations.

Chiral HPLC allowed us to separate and characterize the stereoisomers of **CC1**. The chromatogram of **CC1** (Figure 3A) shows both the pair of enantiomers and the meso isomer. In the chromatogram, peaks **A** and **C** have equal integrated intensity and therefore represent the enantiomeric pair. A third peak, **B**, corresponds to the meso stereoisomer. Using HPLC with a circular dichroism (CD) detector, we were able to confirm this assignment (Figure 3B). The two peaks in the chromatogram assigned to the two enantiomers gave opposite CD signals (225−800 nm, Figure 3B,C). As anticipated, the peak assigned to the meso compound had no detectable CD signal.

It is interesting that **A** and **C** interconvert at room temperature, albeit not directly; the interconversion requires the intermediacy of **B**, the meso compound. To confirm the intermediacy of **B**, we used preparative HPLC. We obtained a pure fraction of **C** and immediately reinjected it into the HPLC and monitored for appearance of the **A** and **B** stereoisomers

DOI: 10.1021/jacs.5b05698
J. Am. Chem. Soc. 2015, 137, 9982−9987

(Figure S3). Within 20 min, the concentration of **B** had already reached 62% of its equilibrium value, yet that of **A** had reached only 8% of its equilibrium value. After 2 h at room temperature, all peaks had reached their equilibrium intensities. This result is remarkable because it suggests the mode of isomerization is a PDI "intramolecular somersault" in which one of the PDIs rotates around its transverse axis, thereby moving one of its diimide heads through the plane of the cavity. This somersault converts a chiral molecule into an achiral one and vice versa. Figure 3D shows a schematic of this conversion process between **A** and **B**.

We were also interested in the rate of interconversion, and we used variable-temperature HPLC to study this process. Maintaining the temperature of both the HPLC column and the sample at 0 °C, we analyzed the freshly isolated meso isomer, **B**, monitoring its conversion to both of the enantiomers (**A**/**C**) over time. Figure S4B shows the natural log of the diastereomeric excess as a function of time. If we assume that this process is a simple first-order reaction, the rate constant was ~10^{-4} s^{-1} at 0 °C. It is difficult to relate this rate to other macrocycles, given there have been just a few kinetic studies concerning the racemization of conjugated belt-like compounds.[6,16,17] Yet, we see experimentally that equilibrium is reached within 2 h at room temperature as discussed above.

The electronic properties of **CC1** can be appreciated by consideration of its UV–vis absorption spectrum (Figure 4),

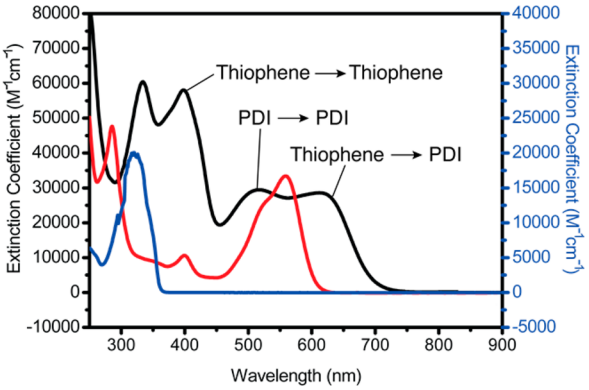

Figure 4. UV–vis absorption spectrum of **CC1** (black line), 5,5′-bis(trimethylstannyl)-2,2′-bithiophene (blue), and **2** (red) in CH_2Cl_2 (concentration = 1.6 × 10^{-5}, 1.3 × 10^{-4}, and 1.8 × 10^{-5} M, respectively, path length = 1.0 cm). The blue trace is plotted with respect to the right ordinate, and the black and red traces are plotted with respect to the left ordinate.

particularly when compared to the spectra of its constituent parts, viz., a helically deformed PDI (**2**) and a bithiophene derivative. **CC1** retains the shorter-wavelength absorptions (~300–400 nm) characteristic of bithiophene and the intermediate-wavelength absorptions (~450–550 nm) characteristic of PDIs, but a new, strong absorption band appears at longer wavelength (~550–700 nm). The optical gap is estimated to be 1.8 eV from the absorption band edge. It is the addition of this latter band that completes the absorption of the visible and renders **CC1** black in color.

We used quantum chemical calculations (time-dependent DFT) to characterize the low-lying excited states of **CC1** and found that while there is little charge transfer from the electron-rich thiophenes to the electron-accepting PDIs in the ground state of the molecule, there is such charge transfer in the lowest-energy excited states: the long-wavelength absorptions are best viewed as forming bithiophene-to-PDI charge transfer states (Figure S5). We also studied the energetics of the frontier orbitals of **CC1** using electrochemistry (see Figure S6). The onset of the first oxidation (0.58 V) and reduction (−1.07 V) peaks relative to Fc/Fc^+ provides an estimate of the HOMO–LUMO gap (1.6 eV). Similar to other aryl-substituted PDI compounds, **CC1** has one oxidation and two one-electron reductions, revealing that the PDIs within **CC1** retain their ability to accept two electrons.[44,52]

CONCLUSIONS

In this study, we have described a new class of fully conjugated macrocycles that incorporate donor and acceptors subunits to form a chiral conjugated corral. **CC1** is the first example of a conjugated macrocycle with alternating aromatic subunits in an –A–B–A–B– pattern. These new macrocycles possess an interesting topology and useful electronic properties that are a result of the pattern written into the cycle. The corral's unusual electronic structure provides a small HOMO/LUMO gap and broad absorbance across the entire visible light spectrum. Excited-state DFT calculations reveal intramolecular charge transfer in the frontier orbitals. Not only does the corral's rich conformational dynamics allow for the interconversion of this macrocycle between chiral and achiral forms, but this easy propensity for shape-shifting offers the appealing opportunity for sterically forgiving host–guest chemistry. This unusual set of properties makes the corrals exciting new candidates for use in energy applications such as photovoltaics.

ASSOCIATED CONTENT

Supporting Information

Experimental procedures for the synthesis and characterization of **CC1** and precursors. UV–vis spectroscopy, cyclic voltammetry, VT-NMR, HPLC, crystallographic data (CIF), and computational details. The Supporting Information is available free of charge on the ACS Publications website at DOI: 10.1021/jacs.5b05698.

AUTHOR INFORMATION

Corresponding Authors

*hexing-li@shnu.edu.cn
*senksong@msn.com
*fwn2@columbia.edu
*mls2064@columbia.edu
*cn37@columbia.edu

Author Contributions

⊥M.B. and B.F. contributed equally to this work.

Notes

The authors declare no competing financial interest.

ACKNOWLEDGMENTS

We thank Qishui (Tracy) Chen, Timothy Su, Ying Wu, and Xiaoyang Zhu for insightful discussions. Primary support for this project was provided by the Chemical Sciences, Geosciences and Biosciences Division, Office of Basic Energy Sciences, U.S. Department of Energy (DOE) under award number DE-FG02-01ER15264. We would also like to thank Columbia University's Shared Materials Characterization Lab for use of the equipment essential to the research. We thank NSFC (21473113), Shanghai Municipal Science and Technology Commission (no. 12nm0504000), Program for Professor

DOI: 10.1021/jacs.5b05698
J. Am. Chem. Soc. 2015, 137, 9982–9987

of Special Appointment (Eastern Scholar) at Shanghai Institutions of Higher Learning (no. 2013-57), "Shuguang Program" supported by Shanghai Education Development Foundation and Shanghai Municipal Education Commission, Program for Changjiang Scholars and Innovative Research Team in University (IRT1269), and International Joint Laboratory on Resource Chemistry(IJLRC) for financial support.

REFERENCES

(1) Jasti, R.; Bhattacharjee, J.; Neaton, J. B.; Bertozzi, C. R. *J. Am. Chem. Soc.* **2008**, *130*, 17646.
(2) Evans, P. J.; Darzi, E. R.; Jasti, R. *Nat. Chem.* **2014**, *6*, 404.
(3) Omachi, H.; Matsuura, S.; Segawa, Y.; Itami, K. *Angew. Chem., Int. Ed.* **2010**, *49*, 10202.
(4) Segawa, Y.; Miyamoto, S.; Omachi, H.; Matsuura, S.; Šenel, P.; Sasamori, T.; Tokitoh, N.; Itami, K. *Angew. Chem., Int. Ed.* **2011**, *50*, 3244.
(5) Segawa, Y.; Šenel, P.; Matsuura, S.; Omachi, H.; Itami, K. *Chem. Lett.* **2011**, *40*, 423.
(6) Omachi, H.; Segawa, Y.; Itami, K. *Org. Lett.* **2011**, *13*, 2480.
(7) Omachi, H.; Segawa, Y.; Itami, K. *Acc. Chem. Res.* **2012**, *45*, 1378.
(8) Ishii, Y.; Nakanishi, Y.; Omachi, H.; Matsuura, S.; Matsui, K.; Shinohara, H.; Segawa, Y.; Itami, K. *Chem. Sci.* **2012**, *3*, 2340.
(9) Yamago, S.; Watanabe, Y.; Iwamoto, T. *Angew. Chem., Int. Ed.* **2010**, *49*, 757.
(10) Iwamoto, T.; Watanabe, Y.; Sadahiro, T.; Haino, T.; Yamago, S. *Angew. Chem., Int. Ed.* **2011**, *50*, 8342.
(11) Iwamoto, T.; Watanabe, Y.; Sakamoto, Y.; Suzuki, T.; Yamago, S. *J. Am. Chem. Soc.* **2011**, *133*, 8354.
(12) Kayahara, E.; Sakamoto, Y.; Suzuki, T.; Yamago, S. *Org. Lett.* **2012**, *14*, 3284.
(13) Iwamoto, T.; Kayahara, E.; Yasuda, N.; Suzuki, T.; Yamago, S. *Angew. Chem., Int. Ed.* **2014**, *53*, 6430.
(14) Kayahara, E.; Patel, V. K.; Yamago, S. *J. Am. Chem. Soc.* **2014**, *136*, 2284.
(15) Yamago, S.; Kayahara, E.; Iwamoto, T. *Chem. Rec.* **2014**, *14*, 84.
(16) Hitosugi, S.; Nakanishi, W.; Isobe, H. *Chem. - Asian J.* **2012**, *7*, 1550.
(17) Hitosugi, S.; Yamasaki, T.; Isobe, H. *J. Am. Chem. Soc.* **2012**, *134*, 12442.
(18) O'Sullivan, M. C.; Sprafke, J. K.; Kondratuk, D. V.; Rinfray, C.; Claridge, T. D. W.; Saywell, A.; Blunt, M. O.; O'Shea, J. N.; Beton, P. H.; Malfois, M.; Anderson, H. L. *Nature* **2011**, *469*, 72.
(19) Neuhaus, P.; Cnossen, A.; Gong, J. Q.; Herz, L. M.; Anderson, H. L. *Angew. Chem., Int. Ed.* **2015**, *54*, 7344.
(20) Jiang, H. W.; Tanaka, T.; Mori, H.; Park, K. H.; Kim, D.; Osuka, A. *J. Am. Chem. Soc.* **2015**, *137*, 2219.
(21) Nishihara, T.; Segawa, Y.; Itami, K.; Kanemitsu, Y. *J. Phys. Chem. Lett.* **2012**, *3*, 3125.
(22) Camacho, C.; Niehaus, T. A.; Itami, K.; Irle, S. *Chem. Sci.* **2013**, *4*, 187.
(23) Alvarez, M. P.; Burrezo, P. M.; Kertesz, M.; Iwamoto, T.; Yamago, S.; Xia, J. L.; Jasti, R.; Navarrete, J. T. L.; Taravillo, M.; Baonza, V. G.; Casado, J. *Angew. Chem., Int. Ed.* **2014**, *53*, 7033.
(24) The smallest HOMO/LUMO gap in a **CPP** is seen in [5]-CPP, the smallest CPP synthesized to date. The HOMO/LUMO gap from calculations is 2.34 eV. See refs 2 and 12.
(25) Havinga, E. E.; ten Hoeve, W.; Wynberg, H. *Polym. Bull.* **1992**, *29*, 119.
(26) Havinga, E. E.; ten Hoeve, W.; Wynberg, H. *Synth. Met.* **1993**, *55*, 299.
(27) Leriche, P.; Frère, P.; Cravino, A.; Alévêque, O.; Roncali, J. *J. Org. Chem.* **2007**, *72*, 8332.
(28) Anthony, J. E.; Facchetti, A.; Heeney, M.; Marder, S. R.; Zhan, X. W. *Adv. Mater.* **2010**, *22*, 3876.
(29) Nolde, F.; Pisula, W.; Müller, S.; Kohl, C.; Müllen, K. *Chem. Mater.* **2006**, *18*, 3715.
(30) Zhong, Y.; Kumar, B.; Oh, S.; Trinh, M. T.; Wu, Y.; Elbert, K.; Li, P. P.; Zhu, X. Y.; Xiao, S. X.; Ng, F.; Steigerwald, M. L.; Nuckolls, C. *J. Am. Chem. Soc.* **2014**, *136*, 8122.
(31) Ball, M.; Zhong, Y.; Wu, Y.; Schenck, C.; Ng, F.; Steigerwald, M.; Xiao, S. X.; Nuckolls, C. *Acc. Chem. Res.* **2015**, *48*, 267.
(32) Zhou, E. J.; Cong, J. Z.; Wei, Q. S.; Tajima, K.; Yang, C. H.; Hashimoto, K. *Angew. Chem., Int. Ed.* **2011**, *50*, 2799.
(33) Li, C.; Wonneberger, H. *Adv. Mater.* **2012**, *24*, 613.
(34) Sharenko, A.; Proctor, C. M.; van der Poll, T. S.; Henson, Z. B.; Nguyen, T.-Q.; Bazan, G. C. *Adv. Mater.* **2013**, *25*, 4403.
(35) Cai, Y.; Huo, L.; Sun, X.; Wei, D.; Tang, M.; Sun, Y. *Adv. Energy Mater.* **2015**, *5*, 1500032.
(36) Huo, L. J.; Zhou, Y.; Li, Y. F. *Macromol. Rapid Commun.* **2008**, *29*, 1444.
(37) Yan, Q. F.; Zhao, D. H. *Org. Lett.* **2009**, *11*, 3426.
(38) Roncali, J. *Chem. Rev.* **1992**, *92*, 711.
(39) Roncali, J. *Macromol. Rapid Commun.* **2007**, *28*, 1761.
(40) Zhang, F.; Götz, G.; Winkler, H. D. F.; Schalley, C. A.; Bäuerle, P. *Angew. Chem., Int. Ed.* **2009**, *48*, 6632.
(41) Stille, J. K. *Angew. Chem., Int. Ed. Engl.* **1986**, *25*, 508.
(42) Zhang, J. X.; Singh, S.; Hwang, D. K.; Barlow, S.; Kippelen, B.; Marder, S. R. *J. Mater. Chem. C* **2013**, *1*, 5093.
(43) Rohr, U.; Kohl, C.; Müllen, K.; van de Craats, A.; Warman, J. *J. Mater. Chem.* **2001**, *11*, 1789.
(44) Chao, C.-C.; Leung, M.-K.; Su, Y. O.; Chiu, K.-Y.; Lin, T.-H.; Shieh, S.-J.; Lin, S.-C. *J. Org. Chem.* **2005**, *70*, 4323.
(45) The 1,7-dibromo-PDI is synthesized from the parent anhydride according to known procedures. See ref 30.
(46) The 1,6- and 1,7-regioisomers are present in the parent dibromo-PDI in a 1:5 ratio and, as a result, are present after the Stille coupling reaction to form **2**. However, we are able to separate the regioisomers with chromatography and proceed with solely the 1,7-isomer to form **3**. Details are contained the Supporing Information.
(47) Eaborn, C.; Odell, K. J.; Pidcock, A. *J. Chem. Soc., Dalton Trans.* **1978**, 357.
(48) We use branched undecyl side chains in order to enhance the solubility of the macrocycle. See refs 29 and 30.
(49) Zhong, Y.; Trinh, M. T.; Chen, R. S.; Wang, W.; Khlyabich, P. P.; Kumar, B.; Xu, Q. Z.; Nam, C.-Y.; Sfeir, M. Y.; Black, C.; Steigerwald, M. L.; Loo, Y.-L.; Xiao, S. X.; Ng, F.; Zhu, X.-Y.; Nuckolls, C. *J. Am. Chem. Soc.* **2014**, *136*, 15215.
(50) Branched alkane side chains rotate slowly on the NMR time scale, resulting in broadening of some PDI resonances. See: Rajasingh, P.; Cohen, R.; Shirman, E.; Shimon, L. J. W.; Rybtchinski, B. *J. Org. Chem.* **2007**, *72*, 5973.
(51) See Supporting Information for the X-ray crystal structure of *N*,*N*′-di-(6-undecyl)-1,7-di(4-bromophenyl)perylene-3,4:9,10-tetracarboxylic diimide (Figure S2) and the .cif file.
(52) Goretzki, G.; Davies, E. S.; Argent, S. P.; Warren, J. E.; Blake, A. J.; Champness, N. R. *Inorg. Chem.* **2009**, *48*, 10264.
(53) Samdal, S.; Samuelsen, E. J.; Volden, H. V. *Synth. Met.* **1993**, *59*, 259.
(54) Quattrocchi, C.; Lazzaroni, R.; Brédas, J. L. *Chem. Phys. Lett.* **1993**, *208*, 120.
(55) Capozzi, B.; Dell, E. J.; Berkelbach, T. C.; Reichman, D. R.; Venkataraman, L.; Campos, L. M. *J. Am. Chem. Soc.* **2014**, *136*, 10486.
(56) Ito, H.; Mitamura, Y.; Segawa, Y.; Itami, K. *Angew. Chem., Int. Ed.* **2015**, *54*, 159.

DOI: 10.1021/jacs.5b05698
J. Am. Chem. Soc. 2015, 137, 9982−9987